

Supporting Information - Structural and Electronic Properties of Layered Nanoporous Organic Nanocrystals

Isaiah A. Moses^a, Veronica Barone^{*a,b}

^a*Science of Advanced Materials Program, Central Michigan University, Mount Pleasant,
MI 48859*

^b*Department of Physics, Central Michigan University, Mount Pleasant, MI 48859*

Email address: v.barone@cmich.edu (Veronica Barone)*

Preprint submitted to Computational Materials Science

January 12, 2021

1. Stacking in Graphene

In order to test the methodology, we started our study by computing the stacking energy profile in graphene. Exploiting the symmetric properties of the graphene structure, it is sufficient to perform calculations with the **B** layer varying from the coordinate $\mathbf{B}(x+0.0, y+0.0)$ to $\mathbf{B}(x+a/2, y+b \sin \gamma)$ ($a = b$, $\gamma = 60^\circ$) and use the symmetry to obtain the energies for the second half (from $\mathbf{B}(x+a/2, y+b \sin \gamma)$ to $\mathbf{B}(x+a, y+b \sin \gamma)$). For both the stand-alone bilayer structures and the bulk, the **AA** stacking is least stable. Also quite relatively unstable are structures with **B** around $\mathbf{B}(x+a, y)$ and $\mathbf{B}(x+0.5a, y+a\sqrt{3}/2)$. The stacking energy profile is shown in Figure S1 for graphite and in Figure S2 for a stand alone bilayer graphene. Importantly, the most thermodynamically stable stacking obtained for graphite has **B** at $\mathbf{B}(x+0.0, y+1.4)$. This gives the Figure S1 (**AB** stacked top view) where half of the carbon atoms in an hexagon of **B** are directly on top of the empty center of **A**. This scheme, known as the Bernal stacking, is in agreement with experiments [1].

The result of the optimum interlayer separation and the corresponding energy is presented in Table S1. The optimum interlayer separations for the isolated **AA** and Bernal-stacked (**AB**) bilayer graphene are 3.59 and 3.31 Å, respectively, with corresponding interlayer cohesive energies per atom of 21.6 and 26.8 meV/atom. For graphite, the interlayer interaction energy per atom is 42.9 and 55.4 meV/atom for the **AA** and Bernal stackings, respectively, at the corresponding interlayer separation of 3.59 and 3.28 Å. As shown in Table S1, these values are in good agreement with previous work using the same functional [2] as well as experimental values [3, 4].

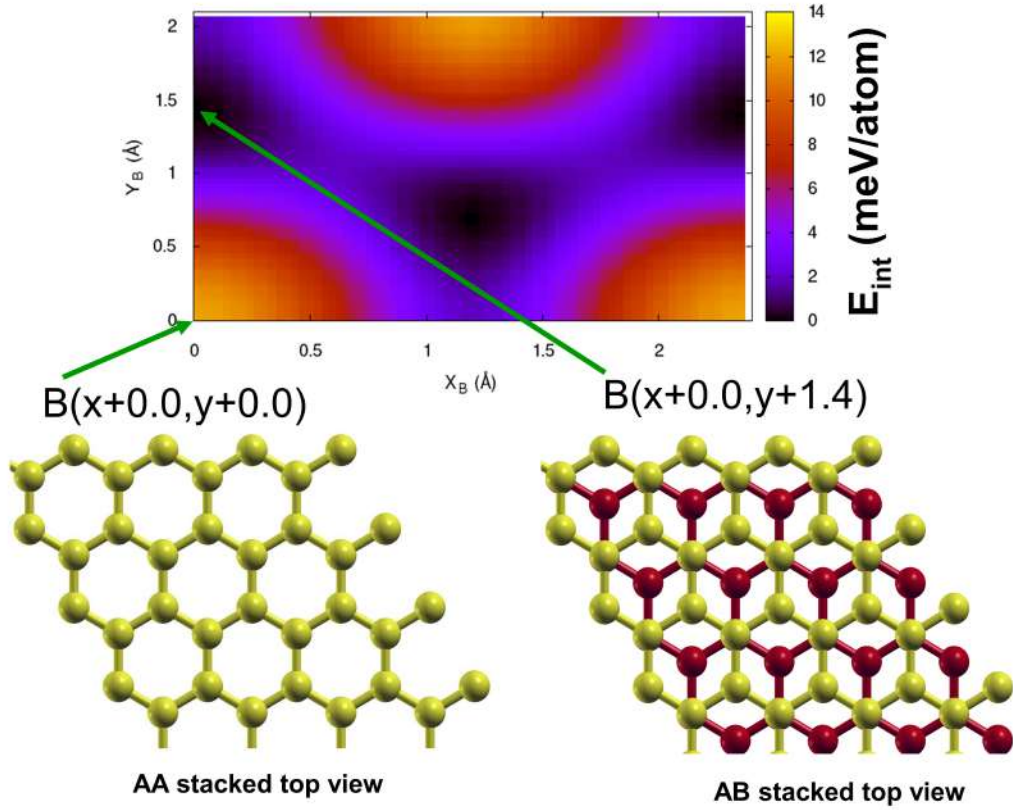


Figure S1: Stacking energy profile in graphite obtained by gliding the top layer with respect to the bottom layer in the (x,y) plane. (X_B, Y_B) is the shift in the top layer relative to the bottom layer. $(X_B=0, Y_B=0)$ corresponds to the **AA** stacking. E_{int} values presented are relative to the most stable stacking configuration.

2. Stacking Energy Profile

The inter-layer interaction energy (E_{int}) profiles are obtained with the interlayer separation fixed at about 3.3 \AA in hexagonal (Figure S3) and oblique structures (Figure S4). The isolated stacking energy profiles are similar to those of the bulk presented in the main paper. The differences are

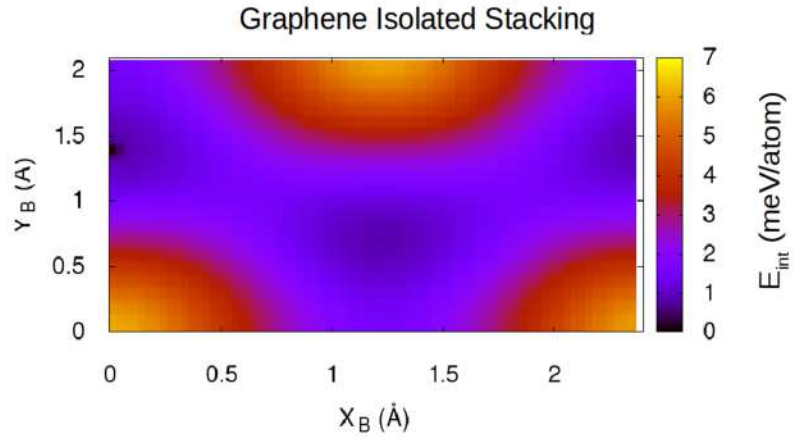


Figure S2: Bilayer stacking energy profile in graphene. The profiles, obtained with interlayer separations fixed at about 3.3 Å. E_{int} values presented are relative to the most stable stacking configuration.

only in the magnitude of the E_{int} with bulk stackings having higher values.

Table S1: The interlayer separation (d) and interaction energy (E_{int}) for stand-alone bilayer graphene and graphite for **AA** and **AB** stackings.

	Stacking	d (Å)	E_{int} (meV/atom)
Isolated	AA	3.59	21.6
	AB	3.31	26.8
Bulk	AA	3.59	42.9
	AB	3.28	55.4
	AB [2]	3.26	54
	AB (exp)	3.336 [3]	52±5 [4]

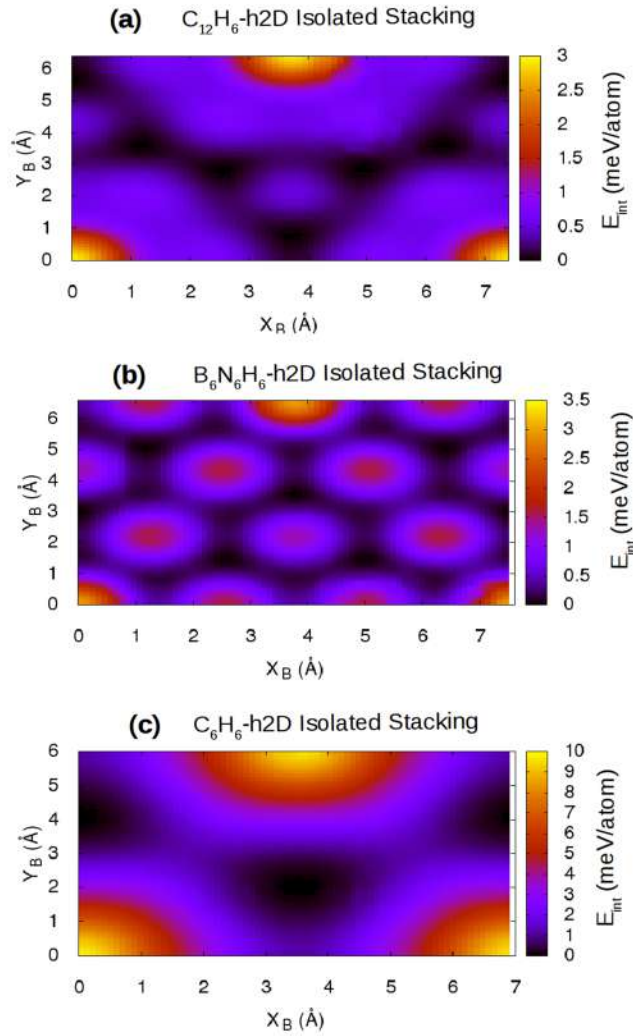


Figure S3: Bilayer stacking energy profile in the hexagonal structures: $C_{12}H_6$ -h2D, $B_6N_6H_6$ -h2D and C_6N_6 -h2D. The profiles, obtained with interlayer separations fixed at about 3.3 \AA . E_{int} values presented are relative to the most stable stacking configuration.

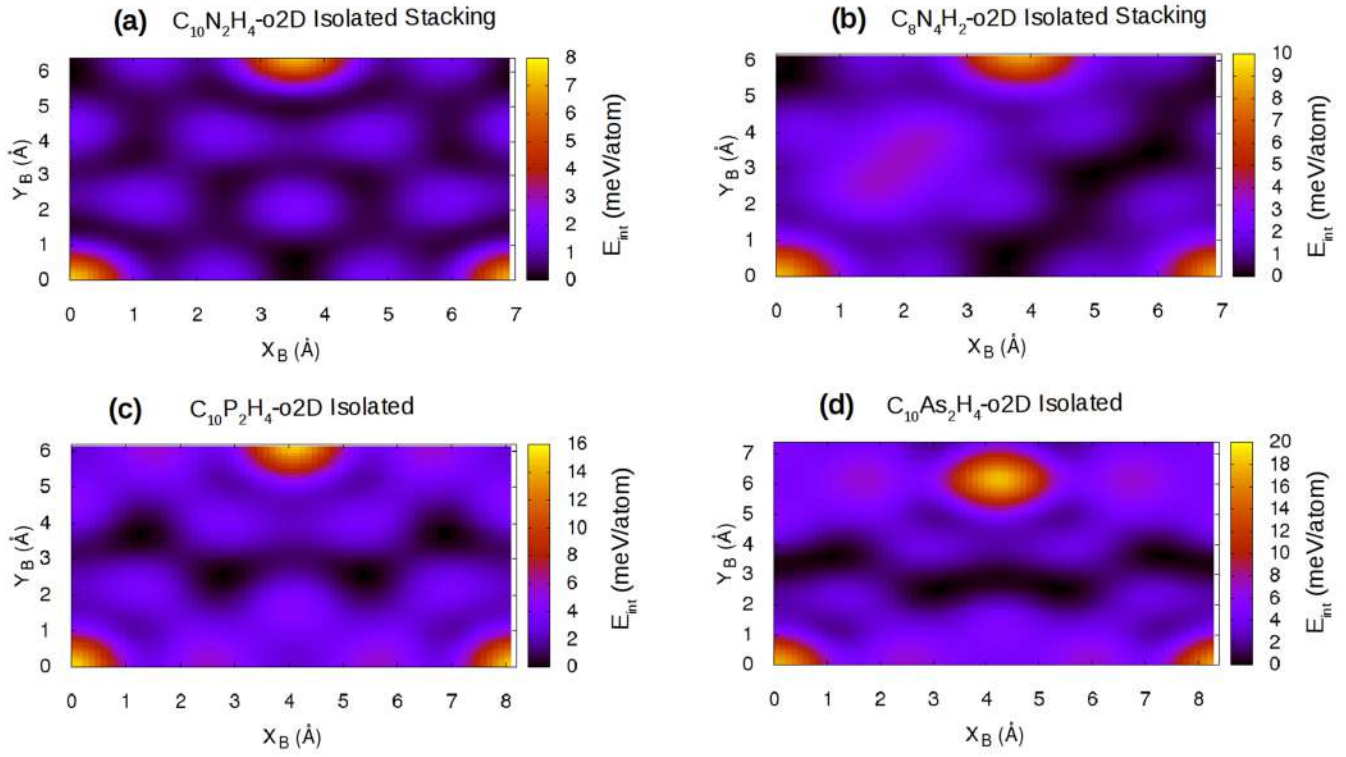


Figure S4: Bilayer stacking energy profile in the oblique structures: $C_{10}N_2H_4$ -o2D, $C_8N_4H_2$ -o2D, $C_{10}P_2H_4$ -o2D, and $C_{10}As_2H_4$ -o2D. The profiles are obtained with fix interlayer separations at about 3.3 \AA . E_{int} values presented are relative to the most stable stacking configuration.

3. The Projected Density of States

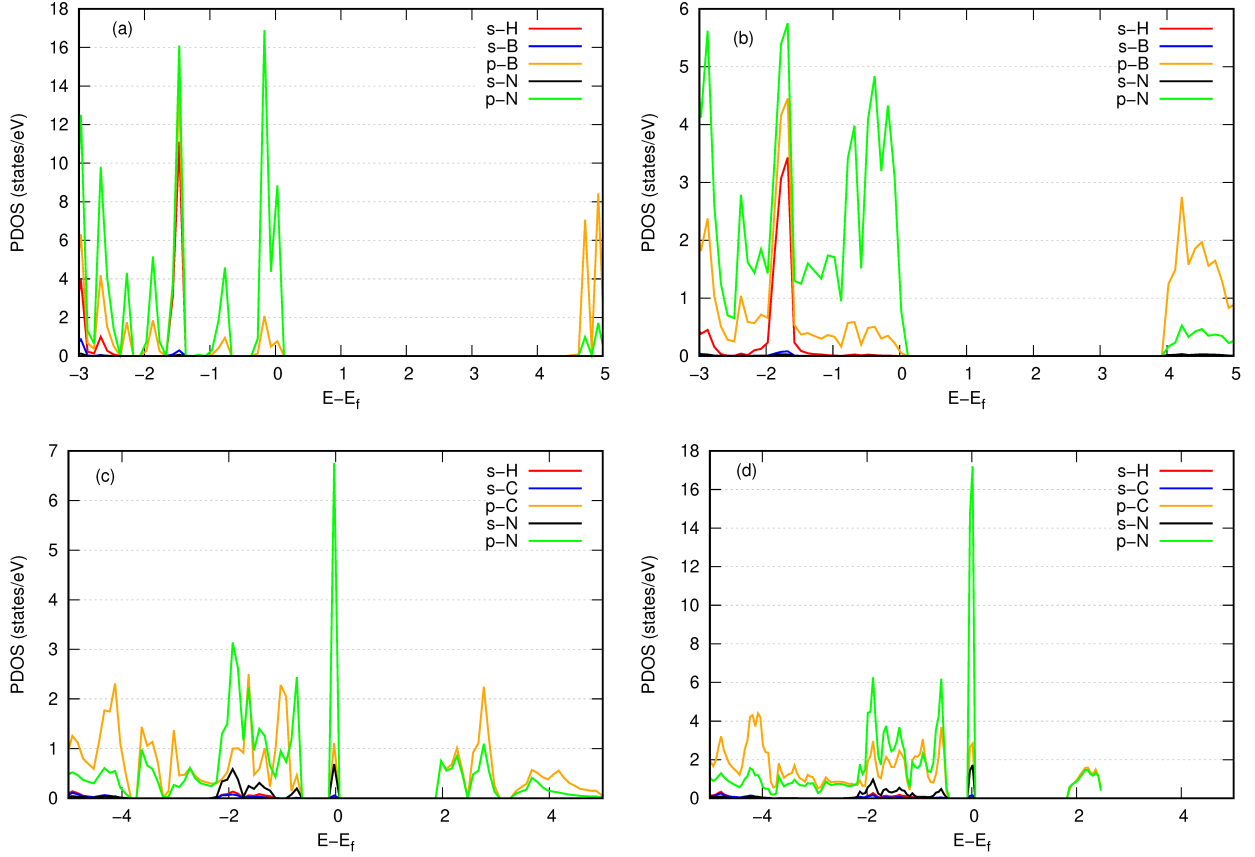


Figure S5: The projected density of states of (a) monolayer $B_6N_6H_6$ -h2D, (b) bulk $B_6N_6H_6$ -h2D, (c) monolayer $C_8N_4H_2$ -o2D and (d) bulk $C_8N_4H_2$ -o2D.

- [1] K. Yan, H. Peng, Y. Zhou, H. Li, Z. Liu, Formation of bilayer bernal graphene: layer-by-layer epitaxy via chemical vapor deposition, *Nano Lett.* 11 (3) (2011) 1106–1110.
- [2] I. Hamada, M. Otani, Comparative van der waals density-functional study of graphene on metal surfaces, *Phys. Rev. B* 82 (15) (2010) 153412.
- [3] Y. Baskin, L. Meyer, Lattice constants of graphite at low temperatures, *Phys. Rev.* 100 (2) (1955) 544.
- [4] R. Zacharia, H. Ulbricht, T. Hertel, Interlayer cohesive energy of graphite from thermal desorption of polyaromatic hydrocarbons, *Phys. Rev. B* 69 (15) (2004) 155406.